Analytical Chemistry, Volume 97, Issue 2, January 2025, pp. 1236-1245
DOI:10.1021/acs.analchem.4c04871

Exploiting the Potential of Spherical PAM-antenna for Enhanced CRISPR-Cas12a: A Paradigm Shift Towards a Universal Amplification-free Nucleic Acid Test Platform

*Jiahui Dai‡[1], Beibei Wu‡[2], Fengxiang Ai[1], Zhugen Yang[3], Yanyan Lu[1], Zinian Cai[1], Kun Zeng[1], Zhen Zhang[1]**

[1]School of the Environment and Safety Engineering, Jiangsu University, Zhenjiang, 212013, China

[2]Zhejiang Provincial Center for Disease Control and Prevention, Hangzhou 310051, China

[3]School of Water, Energy, and Environment, Cranfield University, Milton Keynes, MK43 0AL, UK

*Corresponding author:

E-mail: zhangzhen@ujs.edu.cn

‡ Both authors contributed equally to this paper.

ABSTRACT

The CRISPR-Cas12a system has showed tremendous potential for developing efficient biosensors. Albeit important, current CRISPR-Cas system-based diagnostic technologies (CRISPR-DX) highly rely on additional preamplification procedure to obtain high sensitivity, inevitably leading to the issues such as complicated assay workflow, cross-contamination, etc. Herein, a spherical protospacer-adjacent motif (PAM)-antenna-enhanced CRISPR-Cas12a system is fabricated for universal amplification-free nucleic acid detection with a detection limit of sub-femtomolar, which was further verified using gold-standard real-time quantitative polymerase chain reaction reaction (qPCR) through *Mycobacterium tuberculosis* measurement, demonstrating its good reliability for practical applications. Importantly, its excellent sensitivity is mainly ascribed to high efficiency of target search induced by a localized PAM-enriched microenvironment and improved catalytical activity of Cas12a (up to 4 folds). Our strategy provides some new insights for rapid and sensitive detection of nucleic acid at an amplification-free fashion.

Keywords: Biosensor, Sensor, Rapid detection, Signal amplification, Fluorescence

Published by American Chemical Society. This is the Author Accepted Manuscript issued with: Creative Commons Attribution License (CC:BY 4.0).
The final published version (version of record) is available online at DOI:10.1021/acs.analchem.4c04871. Please refer to any applicable publisher terms of use.

INTRODUCTION

CRISPR-Cas systems, a major component of prokaryotic immune mechanisms[1-4], are widely used in biosensors with the merits of high specificity, efficient signal amplification capacity, and exquisite progarammability[5-11]. Wherein, CRISPR-Cas system-based diagnostic technologies (CRISPR-DX) has gained widespread attention potentially as the next-generation molecular diagnostic technology, benefiting from its efficient trans-cleavage activity and precise RNA-guide nucleic acid recognition[10, 12-18], which could be employed without costly equipment and complex procedures. Actually, the trans-cleavage activity enables indiscriminate degradation of a single-strand DNA (ssDNA) labeled with a pair of fluorophores, and quencher in a high-efficiency fashion to generate readable fluorescence signal after target recognition, which endow the Cas proteins with efficient self-signal amplification and reporting capacities[19-24]. However, the preamplification based analytical techniques always suffer from complicated assay workflow, cross-contaminations, and even false-positive signals[25]. Furthermore, since Cas protein in these methods is always used as an efficient nuclease to capture the presupposed amplification products, its high fidelity and programmable RNA recognition ability were unfortunately ignored.

To overcome the above limitations, the amplification-free detection is implemented by enhancing the CRISPR-Cas system instead of increasing analyte concentrations, promises to omit pre-amplification steps[25-30], which will fit the

CRISPR-Cas system into a portable device for rapid on-site measurement, but current methods mostly focus on the CRISPR trans-cleavage efficiency and signal output improvement[26-28, 30], lacking the prerequisite target recognition process to initiate trans-cleavage activity[31]. Fortunately, evidences indicates that targets search after boosted efficiency will result in the increasing amounts of activated Cas12a, thereby augmenting the collateral effect[20]. Even so, the efficiency of reported methods in target search was estimated of 50%[32], which is insufficient for developing a sensitive detection platform. At the same time, the protospacer-adjacent motif (PAM) was demonstrated of being essential for Cas12a to recognize dsDNA target and subsequent cis- and trans-cleavage activation[31, 33-36], implying that a localized PAM-enriched microenvironment (PAM-antenna) can improve the target recognition performance and trans-cleavage efficiency[24, 37, 38]. Therefore, it is conceivable that the sensitivity of CRISPR-Cas12a system based analytical methods will be obviously elevated.

At the present study, a spherical PAM-antenna was fabricated by decorating 5'-TTTA-3'-present hairpin DNA on magnetic beads (MBs) to design a localized PAM-enriched microenvironment against activator, which will significantly heighten the effective target search efficiency, and make the trans-cleavage event early occurred, even boost catalytical activity of Cas12a regardless of activator sequence (**Scheme 1A**). Accordingly, a novel universal biosensor in an amplification-free fashion was constructed with the aid of smartphone assisted fluorescence reader (**Scheme 1B**), and

its performance was validated of being equivalent to that using qPCR after Mycobacterium tuberculosis (MTB) analysis from clinical samples. We believe that our study is conducive to CRISPR-Cas system based biosensor design and its performance improvement.

EXPERIMENTAL SECTION

Construction of Spherical PAM-antenna

MBs were respectively pre-treated with a washing and magnetic separation procedure to remove the preservative, and then it was suspended in a specialized buffer (10 mM Tris-HCl, 1 mM EDTA, 1 M NaCl, and 0.01%~0.1% Tween-20, pH = 7.5) with a final concentration of 2 mg/mL. Afterwards, FAM and biotin dual-labeled dsDNA were mixed with the above MBs solution at ambient temperature for 1 h with a gently shaking. After magnetic separation and resuspending treatment, the samples were stored at -80℃ for further use. The dual-labeled dsDNA capacity loading capacity of MBs can be calculated through a fluorescence method.

Then, various spherical PAM-antennas with different densities were constructed in a step-by-step modification manner. In brief, after MBs (2 mg/mL, 500 μL) adding to the biotin-modified target dsDNA mimic (or hairpin DNA, 1 μM, 3.75 μL), the solution was incubated at room temperature for 1 h. Then the PAM-richer dsDNA was involved in the above mixture, which was allowed to experience a similar procedure. Ultimately, the spherical PAM-antennas with medium density were magnetically

separated and resuspended into 250 μL buffer, and stored at 4 ℃ for further use. In addition, the spherical PAM-antennas with high (target dsDNA mimic or hairpin DNA, 1 μM, 6.25 μL) and low (target dsDNA mimic or hairpin DNA, 1 μM, 1.25 μL) densities were obtained similarly, unless other indicated.

Real-Time Fluorescence Monitoring Test

A mixture of LbCas12a (20 nM) and the corresponding crRNA with a final ratio of 1:1.25 were incubated about 15 min at room temperature in 1×Tolo Buffer 3 to form Cas12a-crRNA binary complex. After adding spherical PAM-antennas (2 mg/mL), FQ-reporter (800 nM), and activators, or only adding spherical PAM-antennas (2 mg/mL) with FAM/BHQ labeled activators, the test will be carried out using real-time fluorescence scan.

Trans-Cleavage Kinetics Experiments

To measure the trans-cleavage kinetics of Cas12a enzymes, the solution including LbCas12a and the corresponding crRNA were incubated under room temperature in 1 ×Tolo Buffer 3 for reaction about 15 min. After the immediate addition of spherical PAM-antenna (2 mg/mL), FQ reporters (0.01, 0.1, 0.2, 0.5, 1, and 1.5 μM, respectively), and activators, the solution were incubated using three biological replicates in microplate readers for up to 1 h at 37 °C, which was measured by every 30 s (λ_{ex}: 480 nm; λ_{em}: 520 nm). Besides, the results were fitted by linear regression and the initial velocity (V0) plotted against FQ substrate concentration to determine

the Michaelis-Menten equation.

CRISPR-Cas12a-mediated Amplification-Free Fluorescent DNA Assay

The Cas12a-crRNA binary complex was pre-assembled by mixing 20 nM Cas12a and 25 nM crRNA in 1×Tolo buffer 3 in the PCR system at 25 ℃ for reaction, after 15 min, the PAM-antenna-anchored MBs (2 mg/mL), 800 nM FQ-reporter, and DEPC-treated water were added to the above solution. At the same time, the reaction was initiated by the addition of various concentrations of target, and immediately transferred to a microplate reader with the fluorescence signal measurement under the excitation and emission wavelength of 485 and 528 nm, respectively. In addition, the real-time fluorescence was employed to monitor the reaction every 1 s.

Clinical Sample Analysis

This research has been approved by the Medical Ethics Committee of Jiangsu University in China (No. JSDX20230616001). All sputum sample were collected by Zhejiang Provincial Center for Disease Control and Prevention, Hangzhou, China, which were extracted using Saliva DNA Isolation Kit (Norgen Biotek) following the standard protocol and stored at -80℃ until used. Afterwards, the purified genome DNA were heated at 100℃ for 7min and put on ice at once for 5 min to obtained ssDNA[39, 40]， and then, different concentrations of samples were added to the mixture.

RESULTS AND DISCUSSION

Construction of Spherical PAM-Antenna

Fixed quantities of PAM-richer and activator dsDNA were anchored on the surface of MBs through the strong streptavidin-biotin interaction (**Figure 1A**) to fabricate spherical PAM-antenna. In brief, fluorophore-labeled dsDNA was firstly introduced to the system for evaluating the dsDNA loading capacity of MBs. As seen in **Figure 1B**, MBs showed an excellent loading capacity corresponding to the different types of dsDNA (dsDNA with/without overhang, and hairpin DNA). Additionally, spherical PAM-antenna construction was investigated with different ratios of PAM-richer and activator. Besides, **Figure 1C** indicated that the alteration in fluorescence intensity was negligible if only the fluorophore-labeled activators being present, in contrast, the fluorescence intensity progressively elevated with increasing the ratio of fluorophore-labeled PAM (**Figure 1D**), suggesting that the successful construction of different ratios of spherical PAM-antenna.

Effect of Spherical PAM-Antenna on the CRISPR-Cas12a system

Through the necessary procedures of search, recognition, and binding the target sequence, the Cas12a-crRNA binary complex will be changed into a ternary complex, which is essential for activating the cis-cleavage activity of CRISPR-Cas12a system[31]. And the process could be recorded using real-time fluorescence after dsDNA activators were labeled by FAM and BHQ, further revealing the impact of spherical PAM-antenna on the effective target search efficiency within the CRISPR-Cas12a system **(Figure 2A)**. Seen in **Figure 2B,** there were noticeable alterations in fluorescence

intensity (~180s) that occurred prior to the ones observed in the control group (400S) in the presence of spherical PAM-antenna, implying that spherical PAM-antenna may facilitate the search and recognition of Cas12a-crRNA binary complex to the target.

In addition, the trans-cleavage property of activated Cas12a on non-specific ssDNA (custom FQ-reporter) is employed to assess the CRISPR-Cas12a system by spherical PAM-antenna. As depicted in **Figure 2C,** under the PAM-enriched microenvironment, no distinct fluorescence alterations (60 s) was observed compared to the control group (230~280 s) after introducing the Cas12a-crRNA binary complexes, attributed to that more PAM increased the ability for recruiting Cas12a molecules that could diffuse to the target sites, bringing about Cas12a-participated target dsDNA interrogated and cleavage accelerated. Besides, a faster fluorescence signal generation rate was observed, probably due to that the localized PAM microenvironment facilitates the trans-cleavage activity of Cas12a, which was investigated by Michaelis-Menten analysis. As described in **Figure 2D-F**, in comparison with the control group (with a K_{cat}/K_m of 4.1×10^7 s^{-1} M^{-1}), PAM-antenna greatly heightened the catalytic efficiency of Cas12a (K_{cat}/K_m of 8.4×10^7 s^{-1} M^{-1}), indicating that the spherical PAM-antenna could not only improve the cleavage of target dsDNA by Cas12a and the trans-cleavage event, but also enhance the trans-cleavage activity of Cas12a, defined as spherical PAM-antenna induced enhancement effect. Moreover, our investigation showed a shared feature observed using various

forms of dsDNA activators, which could serve as the foundation for an amplification-free ultrasensitive assay design **(Figure 2G)**.

PAM-Enriched Microenvironment Induced the Enhancement Effect

It was anticipated that the enhancement effect of spherical PAM-antenna on Cas12a trans-cleavage benefited from spherical PAM-antenna-modulated microenvironment. As a further investigation, the PAM-richer was adopted in a diffusive manner through removing it from MBs surface, while a dsDNA without PAM sequence was set as the control (**Figure 3A**). The fluorescence results in **Figure 3B** exhibited that the freely diffusive PAM-richer significantly hindered the trans-cleavage activity of Cas12a in a concentration-dependent fashion, while the freely diffusive non-PAM-richer had no significant effect on the trans-cleavage activity of Cas12a, suggesting that the freely diffusive PAM-richer likely acted as competitors to the specific dsDNA activator[41, 42], thus misguiding the Cas12a recognition event. The above results indicated that the confinement of spherical PAM-antenna into a structured microenvironment was all-important for the enhancement of Cas12a activity.

Given that the density and ratio of spherical PAM-antennas will impact on the enhancement effects, they were systematically evaluated. According to **Figures 3C and D**, the most significantly promoted Cas12a trans-cleavage activity was observed under middle density of the spherical PAM-antenna, while that with high density showed a diminished enhancement effect due to a competitive mechanism as above-

mentioned (**Figure S3 and S4)**[41, 42]. In addition, spherical PAM-antenna with low density also showed an inadequate enhancement effect owing to a limited recruitment capability promotability, in consistence with previous literature [41]. Moreover, it was found that the enhancement effect was highly correlated with the ratio of PAM-richer to dsDNA activator (**Fig. 3C and D**). Nevertheless, the higher proportion of PAM-richer and dsDNA activator (> 3:1) actually hindered rather than contributed to the enhancement effect (**Figure S3 and S4**), which may attribute to the certain steric hindrance caused by excess PAM-enricher, as well as the fact that extra PAM-enricher will misguide the Cas12a recognition event toward specific target dsDNA as competitors[24, 41, 42]. These results further confirmed the importance of a localized PAM microenvironment around the dsDNA activator in the improvement of Cas12a activity.

Optimization of the CRISPR-Cas12a Reaction System

Some parameters that potentially influence the performance of the CRISPR-Cas12a detection system were investigated in details, including the concentration of FQ-reporter, Cas12a protein and MBs. As seen in **Figure S5A**, the fluorescence signal demonstrated a dramatically ascending trend with increasing the concentration of FQ-reporter from 100 to 800 nM, then followed by a slight increase from 800 to 1200 nM. To optimize the trade-off between fluorescence signal and timeliness, we selected an 800 nM FQ-reporter as the most suitable setting for the subsequent test. Besides, the concentration of Cas12a protein is another dominant factor for the rise rate of

fluorescence signal because the cleavage accessibility of Cas12a is significant in a concentration-dependent fashion. Moreover, **Figure S5B** showed that the optimized Cas12a protein concentration was identified as 20 nM, based on the negative correlation between the fluorescence signal and Cas12a protein concentration. Higher concentrations of Cas12a protein (> 50 nM) might induce a terminal effect on fluorescence generation. [43]. Owning to the fact that the spherical PAM-antenna was constructed at the MB interface, we speculated that the concentration of MB may affect the microenvironment of the spherical PAM-antenna modulation and subsequent on the CRIPSR-Cas12a system, thus, the effect of MB concentration on the enhancement effect of spherical PAM-antenna was further explored. According to **Figure S5C**, the trans-cleavage rate and activity were maximum when the concentration of MB was increased to 2 mg/mL. Therefore, the concentration of 2 mg/mL for MB was chosen as the optimal level for the creation of the PAM-antenna.

Performance Evaluation of the Spherical PAM-antenna enhanced CRISPR-Cas12a Assay

On the basis of the above findings, an amplification-free analytical assay for *Mycobacterium tuberculosis* (MTB) was constructed as a proof-of-concept to further validate our investigations. Before the detection process for Mycobacterium tuberculosis, the hairpin DNA was designed to contain a partial sequence from DNA genome of Mycobacterium tuberculosis, which can be hybridized with two annealed

transient ssDNA products to form new DNA activator for Cas12a cleavage (**Figure S1**). Upon Cas12a activation, the FQ-reporter can be indiscriminately by the trans-cleavage fashion, thus leading to a considerable fluorescence signal.

Initially, multiple gene fragments and different concentrations of IS6110 gene fragment were introduced to evaluate the quantitative capability of the spherical PAM-antenna-enhanced CRISPR-Cas12a system. As shown in **Figure 4A-C**, regardless of the duration of reaction time (15, 30, and 45 min), the fluorescence signals exhibited a strong correlation with the quantity of IS6110 gene fragment throughout a wide range (1 fM to 1 nM). It is noteworthy that the limit of detection (LOD) of 2.2 fM was obtained, which was significantly higher than the bulk CRISPR-Cas12a system by over 3-4 orders of magnitude. Additionally, we obtained comparable dynamic detection range and LOD for miRNA-10b (18.9 fM) by redesigning the hairpin DNA, demonstrating the versatility of our spherical PAM-antenna-enhanced CRISPR-Cas12a system **(Figure 4F and S1)**.

Besides, the anti-interference capability of the spherical PAM-antenna-enhanced CRISPR-Cas12a system was assessed before measurements by introducing interfering nucleic acids. As observed in Figure 4D, the fluorescence signal of these interference samples showed a negligible discrepancy with that of blank sample, while a similar signal can be seen after the interference samples mixtured, indicating that only the sample containing target DNA induced a considerable higher signal, further

demonstrated its accuracy and specificity. Furthermore, the results in **Figure 4E and 4F** showed that the detection performance in sputum/serum is comparable with that in buffer solution, suggesting a promising application of the spherical PAM-antenna-enhanced CRISPR-Cas12a system in direct biological samples analysis.

Finally, the accuracy of developed method was validated using 42 MTB clinical samples, including 35 positive samples and 24 negative samples **(Figure 5B and 5C)**. The positive predictive agreement (PPA) and negative predictive agreement (NPA) of all detections were determined to be 100% relative to the results of PCR **(Figure 5D and S8)**. Besides, given the limitations of instruments in detecting POC samples, it is crucial to improve portability by utilizing smartphone readings. As depicted in **Figure 5E,** the smartphone application is designed to read the ratio of green to blue intensity (G/B), which is used as the independent variable in the linear scalar equation **(Figure 5F)** to calculate the corresponding dependent variable, further determine the test results. Additionally, to ensure a consistent light source for stimulating the FAM groups and to prevent interference from ambient light, a 3D printed enclosure with the UV light source, power supply, and mechanical parts was constructed to worked in conjunction with the smartphone application. To ascertain the practicality of the aforementioned design, clinical sample No.1 and No.21 were selected as an example **(Figure 5G)**. The analysis results obtained from the smartphone were consistent with the results obtained from the PCR, indicating that a portable analysis of MTB via the

smartphone could be accomplished. Exhibited by Table S1, in comparison with other amplification-free methods, this system showed excellent performances in terms of detection time, sensitivity and universality.

Despite its numerous advantages, the current spherical PAM-antenna enhanced CRISPR-Cas12a system is still subject to certain limitations. A notable drawback is its unvalidated performance in detecting non-nucleic acid targets such as enzymes and small molecules. Additionally, this method cannot simultaneously detect multiple DNA or RNA targets due to the indiscriminate trans-cleavage activity of Cas12a, which would be addressed through the combination of microarray technology with fluorescence coding.

Conclusion

In summary, a novel spherical PAM-antenna-enhanced CRISPR-Cas12a system was developed for amplification-free detection of DNA. This method utilizes PAM-enriched microenvironments to guide the target search and create a local enrichment of Cas12a-crRNA, thereby augmenting the effective target search efficiency and trans-cleavage activity. Furthermore, this enhanced CRISPR-Cas12a system was successfully employed for the ultra-sensitive detection of *Mycobacterium tuberculosis* at sub-femtomolar level without any amplification step, effectively avoiding issues caused by pre-amplification. Consequently, our findings provide new insights into the design of rapid, sensitive, and universal nucleic acid detection platforms, potentially

transforming the landscape of nucleic acid testing by eliminating the need for pre-amplification steps.

CRediT authorship contribution statement

Jiahui Dai: Writing-original draft, Conceptualization, Methodology, Data curation, Visualization. **Beibei Wu:** Conceptualization, Methodology, Software, Data analysis. **Fengxiang Ai**: Software, Samples analysis. **Zhugen Yang**: Software, Samples analysis. **Yanyan Lu**: Software, Samples analysis. **Zinian Cai**: Supervision, Correction of the drafting the work. **Kun Zeng**: Supervision, Correction of the drafting the work. **Zhen Zhang**: Project administration, Validation, Correction of the drafting the work.

Declaration of Competing Interest

The authors declare that they have no known competing financial interests or personal relationships that could have appeared to influence the work reported in this paper

Supporting Information

The Supporting Information is available free of charge at https://pubs.acg.org/doi/10.10121/acs.analchem.XXXXXX. Materials and instruments; oligonucleotides information; optimization of experiment conditions; performance comparisons of our work.

ACKNOWLEDGMENTS

This work was supported by the National Natural Science Foundation of China (Grants No. 22176075 and 22476072), and the Jiangsu Collaborative Innovation Center of Technology and Material of Water Treatment. Besides, ZY also thanks the Leverhulme Trust Research Leadership Awards (RL-2022-041) and the UKRI NERC Fellowship grant (NE/R013349/2).

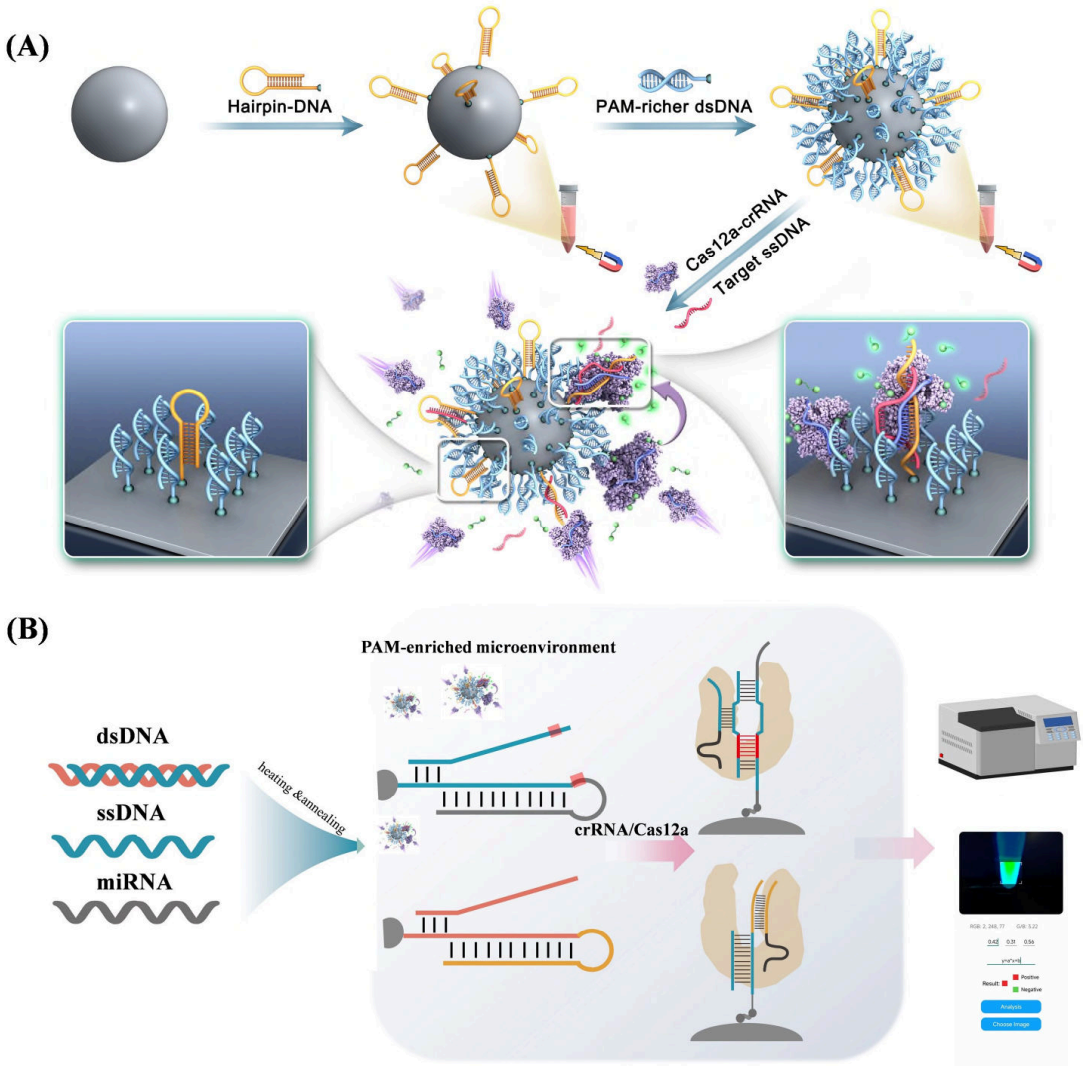
References

(1) Barrangou, P. H. a. R. CRISPR/Cas, the Immune System of Bacteria and Archaea. *Science* **2010**, *327* (5962), 167-170.
(2) Deveau, H.; Garneau, J. E.; Moineau, S. CRISPR/Cas system and its role in phage-bacteria interactions. *Annu Rev Microbiol* **2010**, *64*, 475-493. DOI: 10.1146/annurev.micro.112408.134123.
(3) Sorek, R.; Lawrence, C. M.; Wiedenheft, B. CRISPR-mediated adaptive immune systems in bacteria and archaea. *Annu Rev Biochem* **2013**, *82*, 237-266. DOI: 10.1146/annurev-biochem-072911-172315.
(4) Feng, W.; Newbigging, A. M.; Tao, J.; Cao, Y.; Peng, H.; Le, C.; Wu, J.; Pang, B.; Li, J.; Tyrrell, D. L.; et al. CRISPR technology incorporating amplification strategies: molecular assays for nucleic acids, proteins, and small molecules. *Chem. Sci.* **2021**, *12* (13), 4683-4698.
(5) Yoshizumi Ishino, H. S., Kozo Makino, Mitsuko Amemura, and Atsuo Nakata. Nucleotide Sequence of the iap Gene, Responsible for Alkaline Phosphatase Isozyme Conversion in Escherichia coli, and Identification of the Gene Product. *Journal of Bacteriology* **1987**, *169*, 5429-5433.
(6) Martin Jinek, K. C., Ines Fonfara, Michael Hauer,Jennifer A. Doudna, Emmanuelle Charpentier. A Programmable Dual-RNA–Guided DNA Endonuclease in Adaptive Bacterial Immunity. *Science* **2012**, *337* (6096), 816-821.
(7) Peng, H.; Le, C.; Wu, J.; Li, X. F.; Zhang, H.; Le, X. C. A Genome-Editing Nanomachine Constructed with a Clustered Regularly Interspaced Short Palindromic Repeats System and Activated by Near-Infrared Illumination. *ACS Nano* **2020**, *14* (3), 2817-2826.
(8) Fozouni, P.; Son, S.; Diaz de Leon Derby, M.; Knott, G. J.; Gray, C. N.; D'Ambrosio, M. V.; Zhao, C.; Switz, N. A.; Kumar, G. R.; Stephens, S. I.; et al. Amplification-free detection of SARS-CoV-2 with CRISPR-Cas13a and mobile phone microscopy. *Cell* **2021**, *184* (2), 323-333 e329..
(9) Pardee, K.; Green, A. A.; Takahashi, M. K.; Braff, D.; Lambert, G.; Lee, J. W.; Ferrante, T.; Ma, D.; Donghia, N.; Fan, M.; et al. Rapid, Low-Cost Detection of Zika

Virus Using Programmable Biomolecular Components. *Cell* **2016**, *165* (5), 1255-1266.
(10) Xiong, E.; Jiang, L.; Tian, T.; Hu, M.; Yue, H.; Huang, M.; Lin, W.; Jiang, Y.; Zhu, D.; Zhou, X. Simultaneous Dual-Gene Diagnosis of SARS-CoV-2 Based on CRISPR/Cas9-Mediated Lateral Flow Assay. *Angew Chem Int Ed Engl* **2021**, *60* (10), 5307-5315.
(11) Yang, B.; Kong, J.; Fang, X. Programmable CRISPR-Cas9 microneedle patch for long-term capture and real-time monitoring of universal cell-free DNA. *Nat Commun* **2022**, *13* (1), 3999.
(12) Martin Jinek; Krzysztof Chylinski; Ines Fonfara; Michael Hauer; Jennifer A. Doudna, E. C. A Programmable Dual-RNA–Guided DNA Endonuclease in Adaptive Bacterial Immunity. *Science* **2012**, *337* (6096), 816-821.
(13) Yang, B.; Kong, J.; Fang, X. Programmable CRISPR-Cas9 microneedle patch for long-term capture and real-time monitoring of universal cell-free DNA. *Nat. Commun.* **2022**, *13* (1).
(14) YOSHIZUMI ISHINO, H. S., KOZO MAKINO, ; MITSUKO AMEMURA, A. A. N. Nucleotide Sequence of the iap Gene, Responsible for Alkaline Phosphatase Isozyme Conversion in Escherichia coli, and Identification of the Gene Product. *Journai of Bacteriology* **1987**, *169*, 5429-5433.
(15) Pardee, K.; Green, A. A.; Takahashi, M. K.; Braff, D.; Lambert, G.; Lee, J. W.; Ferrante, T.; Ma, D.; Donghia, N.; Fan, M.; et al. Rapid, Low-Cost Detection of Zika Virus Using Programmable Biomolecular Components. *Cell* **2016**, *165* (5), 1255-1266.
(16) Fozouni, P.; Son, S.; Díaz de León Derby, M.; Knott, G. J.; Gray, C. N.; D'Ambrosio, M. V.; Zhao, C.; Switz, N. A.; Kumar, G. R.; Stephens, S. I.; et al. Amplification-free detection of SARS-CoV-2 with CRISPR-Cas13a and mobile phone microscopy. *Cell* **2021**, *184* (2), 323-333.e329.
(17) Peng, H.; Le, C.; Wu, J.; Li, X.-F.; Zhang, H.; Le, X. C. A Genome-Editing Nanomachine Constructed with a Clustered Regularly Interspaced Short Palindromic Repeats System and Activated by Near-Infrared Illumination. *ACS Nano* **2020**, *14* (3), 2817-2826.
(18) Liu, P.; Lin, Y.; Zhuo, X.; Zeng, J.; Chen, B.; Zou, Z.; Liu, G.; Xiong, E.; Yang, R. Universal crRNA Acylation Strategy for Robust Photo-Initiated One-Pot CRISPR-Cas12a Nucleic Acid Diagnostics. *Angew Chem Int Ed Engl* **2024**, *63* (23), e202401486.
(19) Winston X. Yan; Pratyusha Hunnewell, L. E. A.; Jason M. Carte; Elise Keston-Smith, S. S., Anthony J. Garrity,; Shaorong Chong; Kira S. Makarova; EugeneV.Koonin; David R. Cheng; Scott, D. A. Functionally diverse type V CRISPR-Cas systems. *Science* **2019**, *363*, 88-91.
(20) Janice S. Chen; Enbo Ma; Lucas B. Harrington; Maria Da Costa; Xinran Tian; Joel M. Palefsky; Doudna, J. A. CRISPR-Cas12a target binding unleashes indiscriminate single-stranded DNase activity. *Science* **2018**, *360*, 436-439.
(21) Pickar-Oliver, A.; Gersbach, C. A. The next generation of CRISPR–Cas

technologies and applications. *Nat. Rev. Mol. Cell Biol.* **2019**, *20* (8), 490-507.
(22) Li, S.-Y.; Cheng, Q.-X.; Liu, J.-K.; Nie, X.-Q.; Zhao, G.-P.; Wang, J. CRISPR-Cas12a has both cis- and trans-cleavage activities on single-stranded DNA. *Cell Res.* **2018**, *28* (4), 491-493.
(23) Li, S.-Y.; Cheng, Q.-X.; Wang, J.-M.; Li, X.-Y.; Zhang, Z.-L.; Gao, S.; Cao, R.-B.; Zhao, G.-P.; Wang, J. CRISPR-Cas12a-assisted nucleic acid detection. *Cell Discovery* **2018**, *4* (1).
(24) Zetsche, B.; Gootenberg, Jonathan S.; Abudayyeh, Omar O.; Slaymaker, Ian M.; Makarova, Kira S.; Essletzbichler, P.; Volz, Sara E.; Joung, J.; van der Oost, J.; Regev, A.; et al. Cpf1 Is a Single RNA-Guided Endonuclease of a Class 2 CRISPR-Cas System. *Cell* **2015**, *163* (3), 759-771.
(25) Choi, J.-H.; Lim, J.; Shin, M.; Paek, S.-H.; Choi, J.-W. CRISPR-Cas12a-Based Nucleic Acid Amplification-Free DNA Biosensor via Au Nanoparticle-Assisted Metal-Enhanced Fluorescence and Colorimetric Analysis. *Nano Lett.* **2020**, *21* (1), 693-699.
(26) Nguyen, L. T.; Smith, B. M.; Jain, P. K. Enhancement of trans-cleavage activity of Cas12a with engineered crRNA enables amplified nucleic acid detection. *Nat. Commun.* **2020**, *11* (1).
(27) Ma, J.-Y.; Wang, S.-Y.; Du, Y.-C.; Wang, D.-X.; Tang, A.-N.; Wang, J.; Kong, D.-M. "RESET" Effect: Random Extending Sequences Enhance the Trans-Cleavage Activity of CRISPR/Cas12a. *Anal. Chem.* **2022**, *94* (22), 8050-8057.
(28) Ma, P.; Meng, Q.; Sun, B.; Zhao, B.; Dang, L.; Zhong, M.; Liu, S.; Xu, H.; Mei, H.; Liu, J.; et al. MeCas12a, a Highly Sensitive and Specific System for COVID-19 Detection. *Adv. Sci.* **2020**, *7* (20).
(29) Bruch, R.; Baaske, J.; Chatelle, C.; Meirich, M.; Madlener, S.; Weber, W.; Dincer, C.; Urban, G. A. CRISPR/Cas13a-Powered Electrochemical Microfluidic Biosensor for Nucleic Acid Amplification-Free miRNA Diagnostics. *Adv. Mater.* **2019**, *31* (51).
(30) Choi, J.-H.; Shin, M.; Yang, L.; Conley, B.; Yoon, J.; Lee, S.-N.; Lee, K.-B.; Choi, J.-W. Clustered Regularly Interspaced Short Palindromic Repeats-Mediated Amplification-Free Detection of Viral DNAs Using Surface-Enhanced Raman Spectroscopy-Active Nanoarray. *ACS Nano* **2021**, *15* (8), 13475-13485.
(31) Singh, D.; Mallon, J.; Poddar, A.; Wang, Y.; Tippana, R.; Yang, O.; Bailey, S.; Ha, T. Real-time observation of DNA target interrogation and product release by the RNA-guided endonuclease CRISPR Cpf1 (Cas12a). *Proceedings of the National Academy of Sciences* **2018**, *115* (21), 5444-5449.
(32) Xing, W.; Li, D.; Wang, W.; Liu, J. G.; Chen, C. Conformational dynamics of CasX (Cas12e) in mediating DNA cleavage revealed by single-molecule FRET. *Nucleic Acids Res.* **2024**.
(33) Jeon, Y.; Choi, Y. H.; Jang, Y.; Yu, J.; Goo, J.; Lee, G.; Jeong, Y. K.; Lee, S. H.; Kim, I.-S.; Kim, J.-S.; et al. Direct observation of DNA target searching and cleavage by CRISPR-Cas12a. *Nat. Commun.* **2018**, *9* (1).

(34) Yamano, T.; Zetsche, B.; Ishitani, R.; Zhang, F.; Nishimasu, H.; Nureki, O. Structural Basis for the Canonical and Non-canonical PAM Recognition by CRISPR-Cpf1. *Mol. Cell* **2017**, *67* (4), 633-645.e633.
(35) Swarts, D. C.; van der Oost, J.; Jinek, M. Structural Basis for Guide RNA Processing and Seed-Dependent DNA Targeting by CRISPR-Cas12a. *Mol. Cell* **2017**, *66* (2), 221-233.e224.
(36) Mojica, F. J. M.; Díez-Villaseñor, C.; García-Martínez, J.; Almendros, C. Short motif sequences determine the targets of the prokaryotic CRISPR defence system. *Microbiology* **2009**, *155* (3), 733-740.
(37) Fei Wang; Yaya Hao; Qian Li; Jiang Li; Honglu Zhang; Xueli Zhang; Lihua Wang; Carlos Bustamante, C. F. Programming PAM antennae for efficient CRISPR-Cas9 DNA editing. *Sci. Adv.* **2020**, *6* (19), eaay9948.
(38) Yamano, T.; Nishimasu, H.; Zetsche, B.; Hirano, H.; Slaymaker, Ian M.; Li, Y.; Fedorova, I.; Nakane, T.; Makarova, Kira S.; Koonin, Eugene V.; et al. Crystal Structure of Cpf1 in Complex with Guide RNA and Target DNA. *Cell* **2016**, *165* (4), 949-962.
(39) Yuanfeng, P.; Ruiyi, L.; Qingqing, X.; Xiaofen, C.; Yongqiang, Y.; Zaijun, L. Electrochemical detection of Mycobacterium tuberculosis IS6110 gene fragments based on the gold nanocrystals with uniform morphology and highly exposed high-index facets and target DNA-induced recycling amplification. *Sens. Actuators, B* **2020**, *314*.
(40) Ng, B. Y.; Xiao, W.; West, N. P.; Wee, E. J.; Wang, Y.; Trau, M. Rapid, Single-Cell Electrochemical Detection of Mycobacterium tuberculosis Using Colloidal Gold Nanoparticles. *Anal. Chem.* **2015**, *87* (20), 10613-10618.
(41) Szczelkun, M. D.; Tikhomirova, M. S.; Sinkunas, T.; Gasiunas, G.; Karvelis, T.; Pschera, P.; Siksnys, V.; Seidel, R. Direct observation of R-loop formation by single RNA-guided Cas9 and Cascade effector complexes. *Proceedings of the National Academy of Sciences* **2014**, *111* (27), 9798-9803.
(42) Sternberg, S. H.; Redding, S.; Jinek, M.; Greene, E. C.; Doudna, J. A. DNA interrogation by the CRISPR RNA-guided endonuclease Cas9. *Nature* **2014**, *507* (7490), 62-67.
(43) Yan, H.; Wen, Y.; Tian, Z.; Hart, N.; Han, S.; Hughes, S. J.; Zeng, Y. A one-pot isothermal Cas12-based assay for the sensitive detection of microRNAs. *Nat. Biomed. Eng.* **2023**, *7* (12), 1583-1601.



Scheme 1. Schematic illustration of spherical PAM-antenna for enhancing the trans-cleavage activity of CRISPR-Cas12a system.

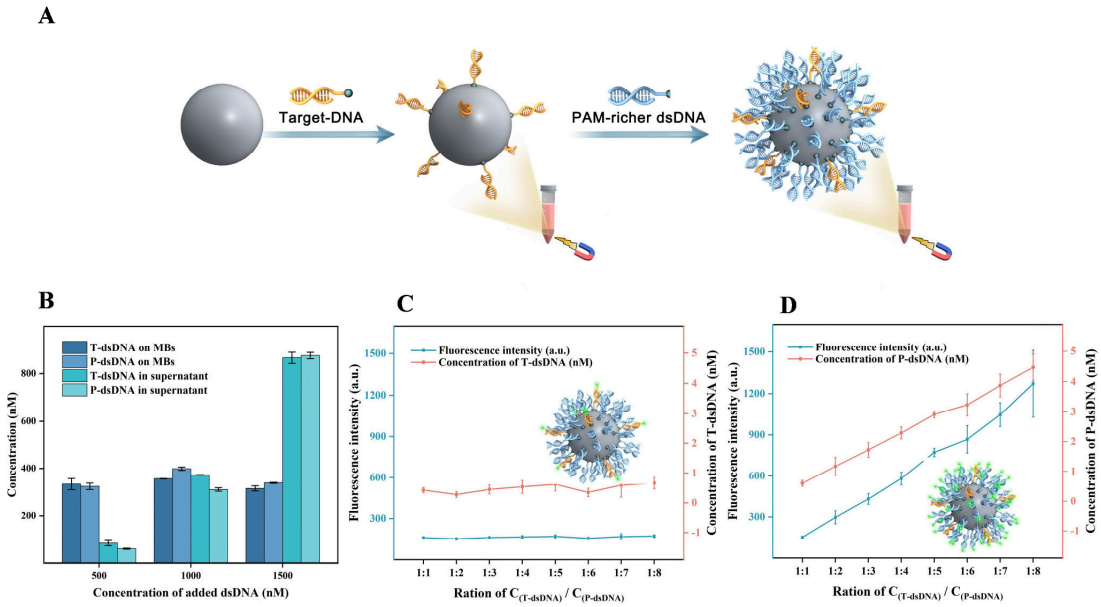


Figure 1. (A) The construction of spherical PAM-antenna by using different types of dsDNA. (B) The evaluation of loading capacity of MB substrate. (C) and (D) The total fluorescence intensity of various ratio of PAM-richer and dsDNA activator and individual percentage of fluorescence intensity. Error bars represented mean± standard deviation, where n = 3 replicates.

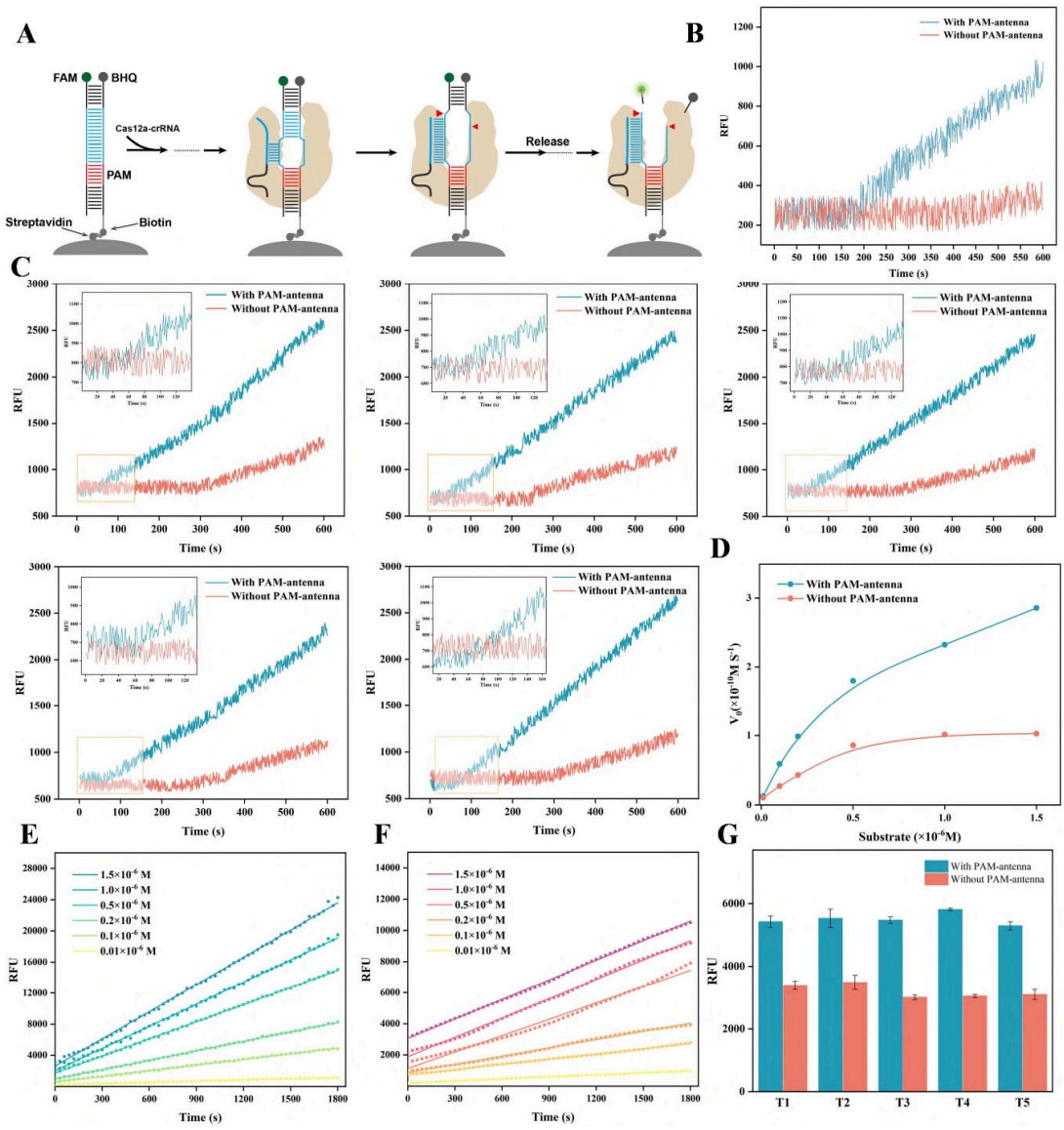


Figure 2. The evaluation of effect of PAM-antenna on Cas12a. (A) Diagram of the cis-cleavage process in CRISPR-Cas12a system. (B) The real-time fluorescence monitoring of cis-cleavage reaction with/without spherical PAM-antenna. C) The real-time fluorescence monitoring of FQ-reporter trans-cleavage reaction for different dsDNA activators with/without spherical PAM-antenna. (D) Enzyme kinetic data of Cas12a with/without spherical PAM-antenna. (E) and (F) Michaelis-Menten plot of

Cas12a in the presence and absence of spherical PAM-antenna. The target concentration was 100 pM. Calculated Kcat, Km and Kcat/Km values report the mean ± s.d., where n = 3 replicates. (F) The investigation of shared property of spherical PAM-antenna enhancement effect by real-time fluorescence. For this investigation, four re-designed dsDNA activators were only employed to replace the above dsDNA activator and other assay procedures are same with normal experimental assay unless otherwise indicated.

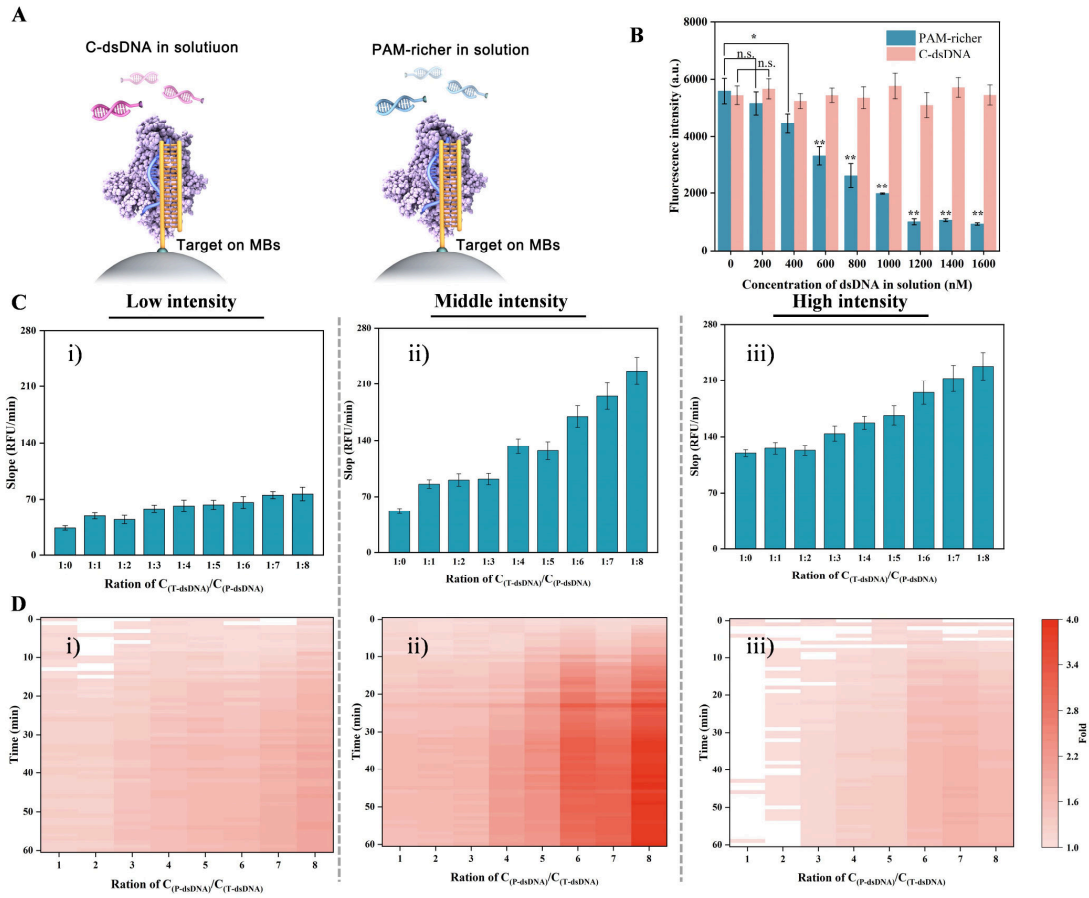


Figure 3. (A) The construction of freely diffuse PAM-richer and C-dsDNA. (B) the fluorescence signal under various concentrations of diffuse PAM-richer and C-dsDNA. The relationship between slope of fluorescence signal (C) and corresponding heat mapping (D) with the density and ratio of PAM-richer. The Error bars mean ± s.d., where n = 3 replicates.

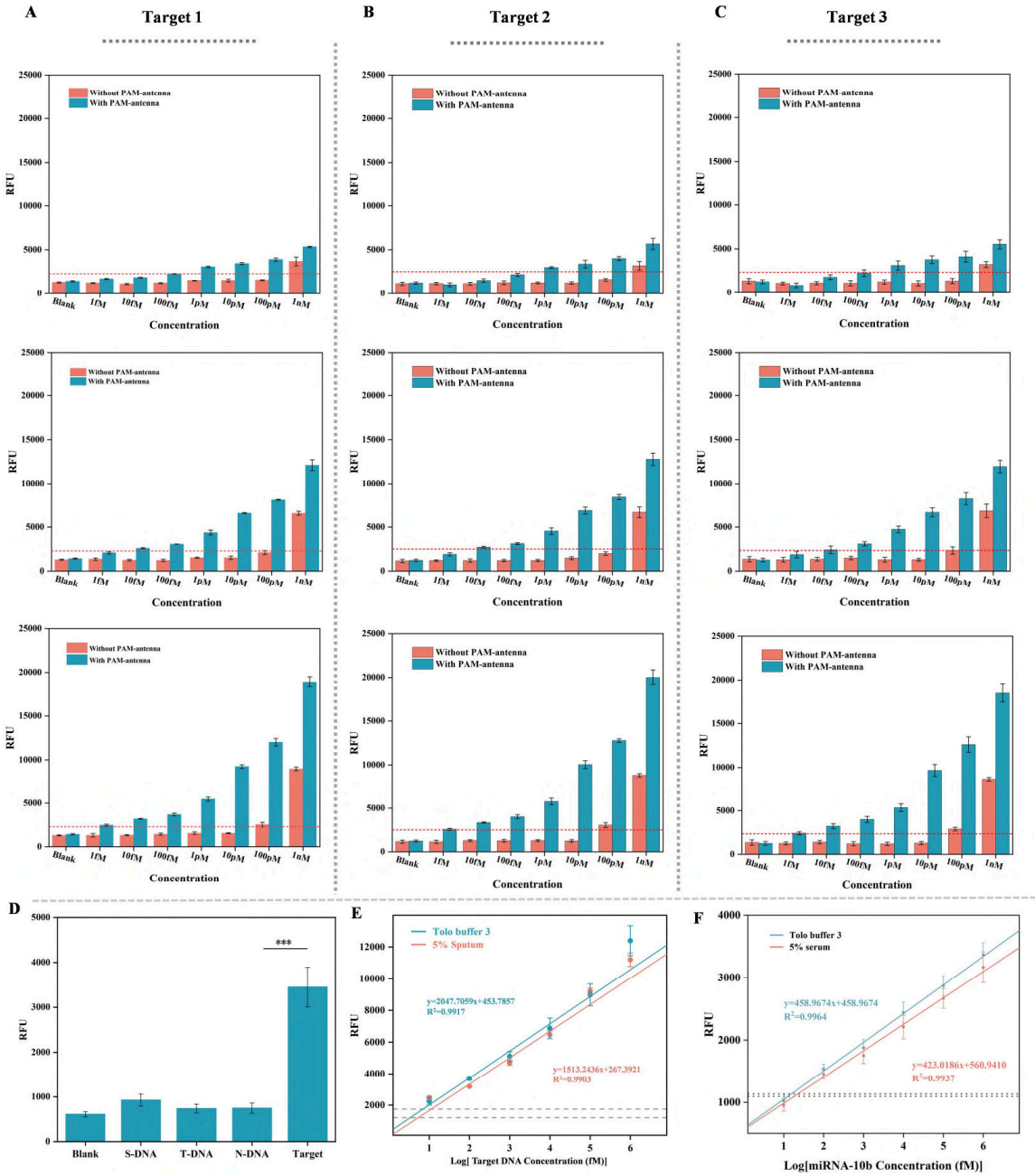
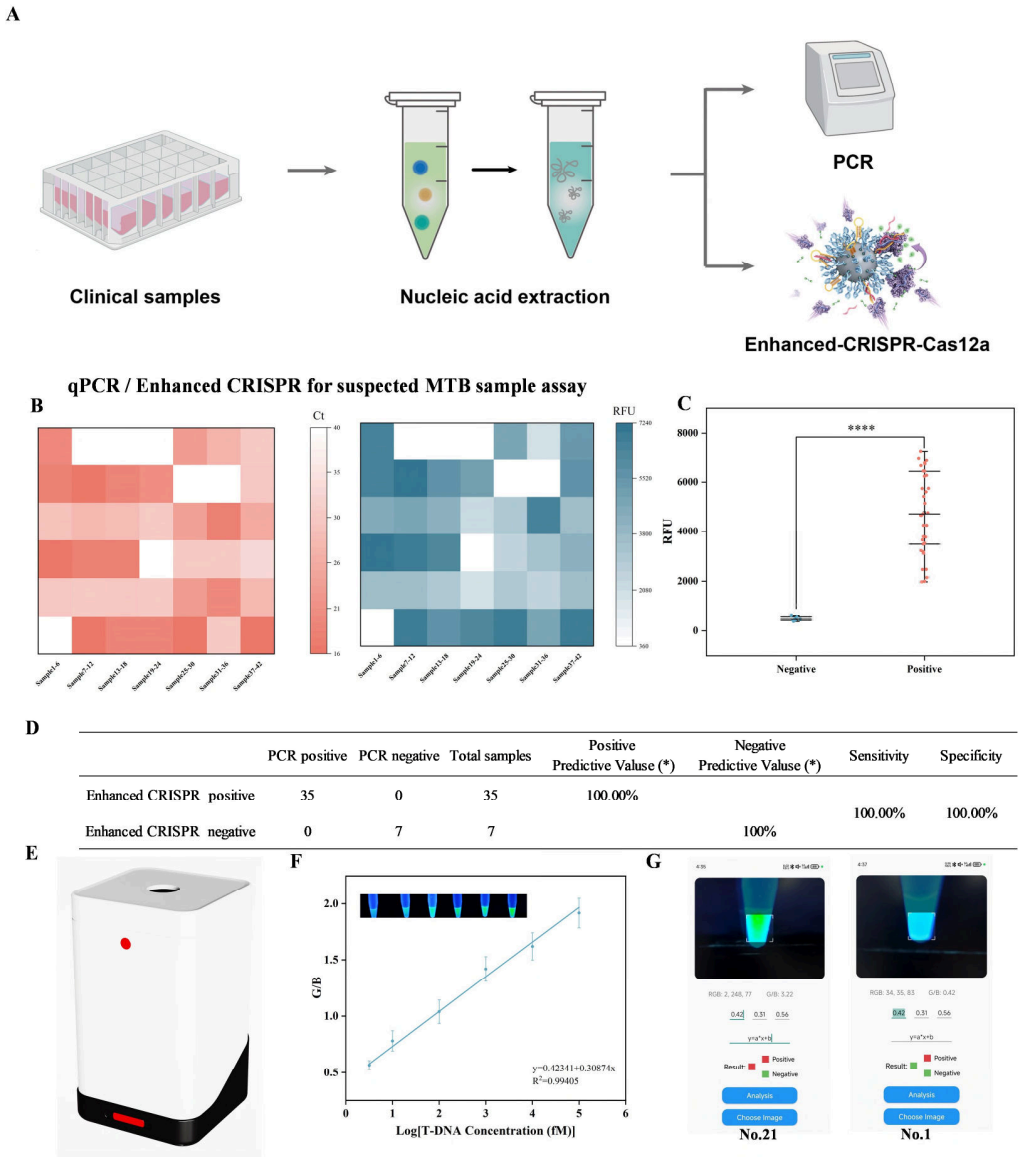


Figure 4. (A-C) Fluorescence intensity of various concentrations of IS6110 gene fragment under different reaction times (15, 30, and 45 min). (D) The specificity evaluation of our Spherical PAM-antenna-enhanced CRISPR-Cas12a system by employing single-base mismatched DNA (S-DNA), two-base mismatched DNA (T-

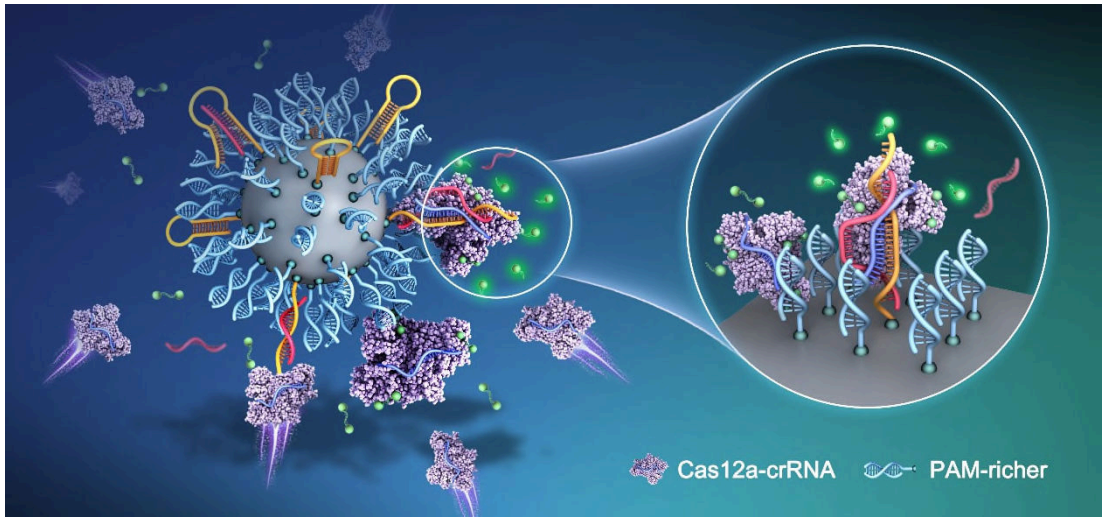
DNA) and non-complementary DNA (N-DNA). (E) The comparison of target DNA measurements in buffer solution and 5% sputum by using our Spherical PAM-antenna-enhanced CRISPR-Cas12a system. Error bars mean ± s.d., where n = 3 replicates. (F) The comparison of miRNA-10b measurements in buffer solution and 5% serum by using our Spherical PAM-antenna-enhanced CRISPR-Cas12a system. Error bars mean ± s.d., where n = 3 replicates.



	PCR positive	PCR negative	Total samples	Positive Predictive Value (*)	Negative Predictive Value (*)	Sensitivity	Specificity
Enhanced CRISPR positive	35	0	35	100.00%		100.00%	100.00%
Enhanced CRISPR negative	0	7	7		100%		

Figure 5. (A) Workflow for clinical sample detection based on PCR and spherical PAM-antenna enhanced CRISPR-Cas12a assay. (B) The heat maps showing the detection results of the 42 samples based on the PCR (top) and the spherical PAM-antenna enhanced CRISPR-Cas12a assay. (C) Scatter plot represents the fluorescence intensity values corresponding to 42 samples detected by spherical PAM-antenna enhanced CRISPR-Cas12a assay. Two-tailed Student's t test; ****, $p < 0.0001$. (D)

Performance characteristics of spherical Pam-antenna-enhanced CRISPR-Cas12a assay (E) The external structure of a 3D printed reader. (F) The linear relationship between the target DNA concentration and G/B. Error bars mean ± s.d., where n = 3 replicates. (G) The image results of clinical samples No.21 and No.1.



Graphical Abstract.

Supporting Information

Exploiting the Potential of Spherical PAM-antenna for Enhanced CRISPR-Cas12a: A Paradigm Shift Towards a Universal Amplification-free Nucleic Acid Test Platform

*Jiahui Dai‡[1], Beibei Wu‡[2], Fengxiang Ai[1], Zhugen Yang[3], Yanyan Lu[1], Zinian Cai[1], Kun Zeng[1], Zhen Zhang[1]**

[1]School of the Environment and Safety Engineering, Jiangsu University, Zhenjiang, 212013, China

[2]Zhejiang Provincial Center for Disease Control and Prevention, Hangzhou 310051, China

[3]School of Water, Energy, and Environment, Cranfield University, Milton Keynes, MK43 0AL, UK

*Corresponding author:

E-mail: zhangzhen@ujs.edu.cn

‡ Both authors contributed equally to this paper.

Chemical and Reagents.

All DNA and RNA oligonucleotides were synthesized and High-Performance Liquid Chromatography (HPLC)-purified by Sangon Biotechnology Co. Ltd. (Shanghai, China), and their detailed sequences information were displayed in Table S1. Streptavidin-modified magnetic beads (MBs, 0.6 μm, 10 mg/mL) were provided by VDO Biotech Co, Ltd. (Suzhou, China). Cas12a endonuclease separated from Lachnospiraceae bacterium ND2006 (LbCas12a) and its storage and reaction buffers were obtained from Tolo Biotech Co, Ltd. (Shanghai, China). Diethyl pyrocarbonate (DEPC)-treated water (DNase, RNase-free), phosphate buffer saline (PBS, PH=7.4), and 1×TE buffer were purchased from Sangon Biotechnology Co. Ltd. (Shanghai, China), in which the DEPC-treated water was utilized as the final solvent of DNA and RNA throughout the experiment.

Apparatus and Measurements.

All fluorescence measurements were carried out on a BioTek synergy H4 multi-mode microplate reader (BioTek Instruments, Inc., VT, USA). Fluorescence spectrum and signals were recorded by using a multi-mode fluorometer microplate-reader, BioTek synergy H4 (USA). The DNA oligonucleotides were thermal treated on a BioRad thermal cycler PTC-100 (USA). Real-time fluorescence intensity was detected using a QuantaMaster 40 (USA). PCR was carried out by Applied Biosystems Veriti 96 Well Thermal Cycler. qPCR was performed in CFX Duet Real-time PCR system (Bio-Rad, USA)

Preparation of the PAM-richer, dsDNA activators and Hairpin DNA

For the preparation of dsDNA, equal amount of ssDNA and its complementary strand (100 μM, 2 μL) was added into a nucleic acid hybridization buffer (100 mM Tris, 120 mM NaCl, 10 mM $MgCl_2$, 100 mM KCl) with a final volume of 200 μL. Subsequently, the above solutions and hairpin DNA solution (100 μM) were annealed at 95 ℃ for 5 min, followed by 55 ℃ for 30 min and slowly cooling down to room temperature (25 ℃), respectively. Hairpin DNA solution (100 μM) was annealed at 95 ℃ for 5 min, followed by 55 ℃ for 30 min and slowly cooling down to room temperature (25 ℃). Finally, all the solutions were stored at 4 ℃ for further use.

PCR and qPCR analysis

The 50 μL PCR reaction mixture contained 25 μL PrimeSTAR Max Premix (2 ×), 0.3 μM forward and reverse primers, and 2 μL genomic DNA. PCR amplification was performed with the following procedure: 95 ℃ for 1 min, followed by 35 cycles of 98 ℃ for 10 s, 55 ℃ for 15 s and 72 ℃ for 5 s. The product at the end of the 35th cycle was kept at 72 ℃ for 5 min and finally stored at 4 ℃ for further use. Then, 1% agarose Gel electrophoresis was used to visualize PCR reaction products.

The 20 μL qPCR reaction mixture contained 10 μL TaqMan Fast qPCR Master Mix (2 ×), 200nM forward and reverse primers, 10 μM probe, and 2 μL genomic DNA. qPCR amplification was performed with the following procedure: 95 ℃ for 3 min, followed by 40 cycles of 94 ℃ for 5 s, and 60 ℃ for 30 s. The above reaction was performed in the CFX Duet Real-time PCR system.

Table S1. The sequences of oligonucleotides used in this work.

Name	Sequence（from 5′ to 3′）
T1-TS	Biotin-TTTT TGC ACG TGT TGT CTC TGA TGT AAA TAG
T2-NTS	CTA AAA TGT AGT CTC TGT TGT GCA CGT
T2-NTS	CTA TTT AGC ATC CCA GAC AGC TTG CCG
T2-TS	Biotin-TTTT CGG CAA GCT GTC TGG GAT GCT AAA TAG
T3-NTS	CTA TTT ATT ACG CAC CCT TTG CCA GAC
T3-TS	Biotin-TTTT GTC TGG CAA AGG GTG CGT AAT AAA TAG
T4-NTS	CTA TTT ATG ATT AAG GCT AAT CCG CTC
T4-TS	Biotin-TTTT GAG CGG ATT CGA CTT AAT CAT AAA TAG
T5-NTS	CTA TTT ACC GAG CAC GGC TTC ACA CAC
T5-TS	Biotin-TTTT GTG TGT GAA GCC GTG CTC GGT AAA TAG
H1-IS6110	Biotin-TTTT GGC TGG CCG GTC GAG CTC GGC CGC GAA GAA AGC CGA TTT ACG CTA TTC GCG CCG AGC TCG ACC GG
H2-IS6110	Biotin-TTTT GGT TAG CCA CAC TTT GCG GGC ACC GTA AAC ACC ATT TAG GCG GCG GTG CCC GCA AAG TGT GGC
H3-IS6110	Biotin-TTTT ATC CTG CGA GCG TAG GCG TCG GTG ACA AAG GCC ATT TAG GCG CTC ACC GAC GCC TAC GCT CGG
crRNA1	UAA UUU CUA CUA AGU GUA GAU CAU CAG AGA CAA CAC GUG CA
crRNA2	UAA UUU CUA CUA AGU GUA GAU GCA UCC CAG ACA GCU UGC CG
crRNA3	UAA UUU CUA CUA AGU GUA GAU UUA CGC ACC CUU UGC CAG AC
crRNA4	UAA UUU CUA CUA AGU GUA GAU UGA UUA AGG CUA AUC CGC UC
crRNA5	UAA UUU CUA CUA AGU GUA GAU CCG AGC ACG GCU UCA CAC AC
crRNA-	UAA UUU CUA CUA AGU GUA GAU UUC GCG GCC GAG CUC

IS6110-1	GAC CG
crRNA-IS6110-2	UAA UUU CUA CUA AGU GUA GAU CGG UCC CCG CAA AGU GUG GC
crRNA-IS6110-3	UAA UUU CUA CUA AGU GUA GAU UCA CCG ACG CCU ACG CUC GC
crRNA-miRNA 10b	UAA UUU CUA CUA AGU GUA GAU UUC AUC UUG GCU UAA ACA CUU UU
PAM-richer-s1	Biotin-TTTT GAAA CAAA GAAA CAAA GAAA CAAA GAAA
PAM-richer-s2	TTTC TTTG TTTC TTTG TTTC TTTG TTTC
FQ-Reporter	FAM-TTATT-BHQ
FAM-S1	CTA AAA TGT AGT CTC TGT TGT GCA CGT-FAM
FAM-PAM-richer-s2	TTTC TTTG TTTC TTTG TTTC TTTG TTTC-FAM
IS6110-1	CGG CTT TCT TCG CGG CCG AGC TCG ACC GGC CAGC
IS6110-2	GGG TGT TTA CGG TGC CCG CAA AGT GTG GCT AACC
IS6110-3	GGC CTT TGT CAC CGA CGC CTA CGC TCG CAG GAT
S-DNA	CGG CTT TCT TCG CGG CCG AGC TCG ACC GGC GAGC
T-DNA	CGG CTT TCT TCG CGG CCG AGA TCG ACC GGC GAGC
N-DNA	ATC GAA AGC AAT TTA GGA CAT AAC CGG TAT TCAT
IS6110-FORWARD	GACCTACTACGACCACATCAAC
IS6110-REVERSE	GTTCAGGGTTAGCCACACTT
IS6110-Probe	FAM-ATGGCGAACTCAAGGA-BHQ

miRNA-10b	GUGUUUAAGCCAAGAUGUCCCAU
Hairpin DNA-miRNA	TTTTATGGGACATCTTGGCTTAAACACTTAAATCCAAAAGTGTTTAAAGCCAAGATGAA

Table S2. Major amplification-free CRISPR/Cas-based detection strategies

Method	Target	Signal read-out	LOD	Sample to answer time (min)	Refs
Optimization of crRNA and signal reporters of the CRISPR-Cas system	HPV-16	FL	10 fM	N.S.	1
	ASFV	FL	1 pM	30	2
	Salmonella enterica	FL	619 CFU	>75	3
Digital-CRISPR ultrasensitive detection platforms	HBV/HPV	FL	5 fM	90	4
	virus's DNAs	FL	17.5 copies per mL	60	5
Signal transducer formation	DENV-4	EC	100 fM	50	6
	HIV	ECL	30 fM	120	7
	PB-19	EC	10 fM	>60	8
	MRSA bacteria *mecA gene*	EC	3.5 fM	90	9
	HPV	EC	30pM	60	10
This method	MTB/miRNA	FL	2.2 fM/18.9 fM	<30	

Table S3. *Ct* values obtained from the detection of 42 clinical Mycobacterium tuberculosis samples by qPCR.

Sample ID	1	2	3	4	5	6	7	8
C_t	--	16.07	17.61	16.21	17.66	16.60	18.53	18.14
Sample ID	9	10	11	12	13	14	15	16
C_t	18.79	18.67	--	20.09	16.38	30.87	--	30.56
Sample ID	17	18	19	20	21	22	23	24
C_t	30.89	--	16.18	32.80	30.05	29.72	29.46	19.84
Sample ID	25	26	27	28	29	30	31	32
C_t	30.53	27.38	--	30.35	28.41	--	30.93	30.87
Sample ID	33	34	35	36	37	38	39	40
	--	22.95	23.39	22.45	19.67	18.29	26.51	27.89
Sample ID	41	42						
	25.37	31.14						

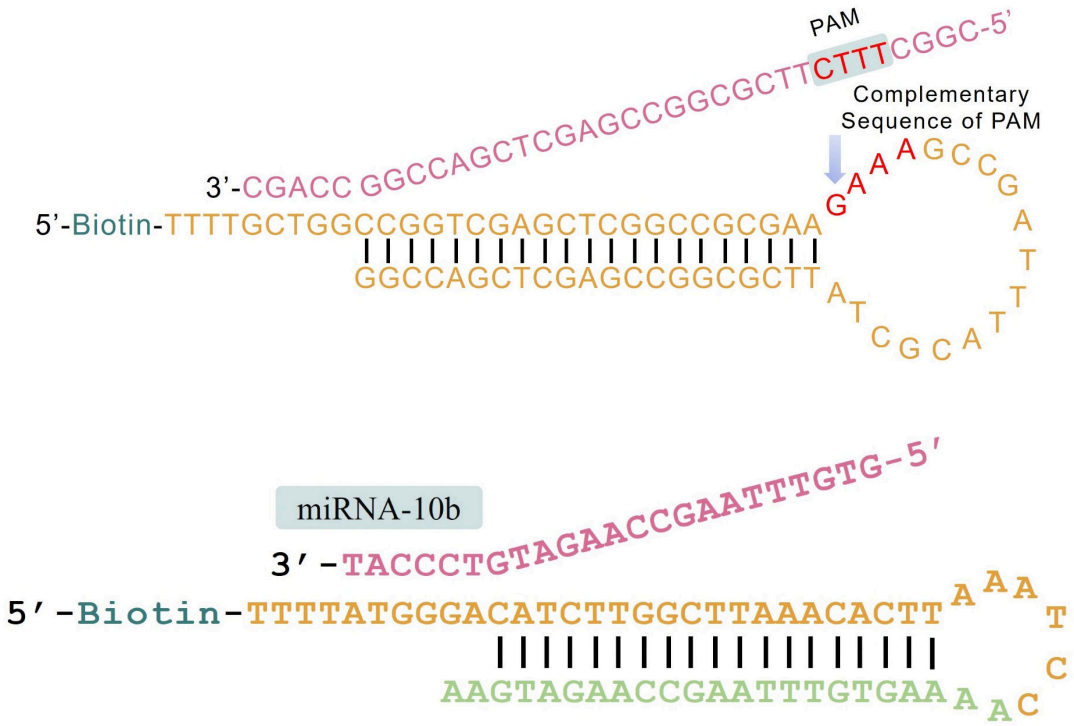


Figure S1. Schematic representation of IS6110 gene fragment/miRNA-10b opens the Hairpin DNA to form an activator.

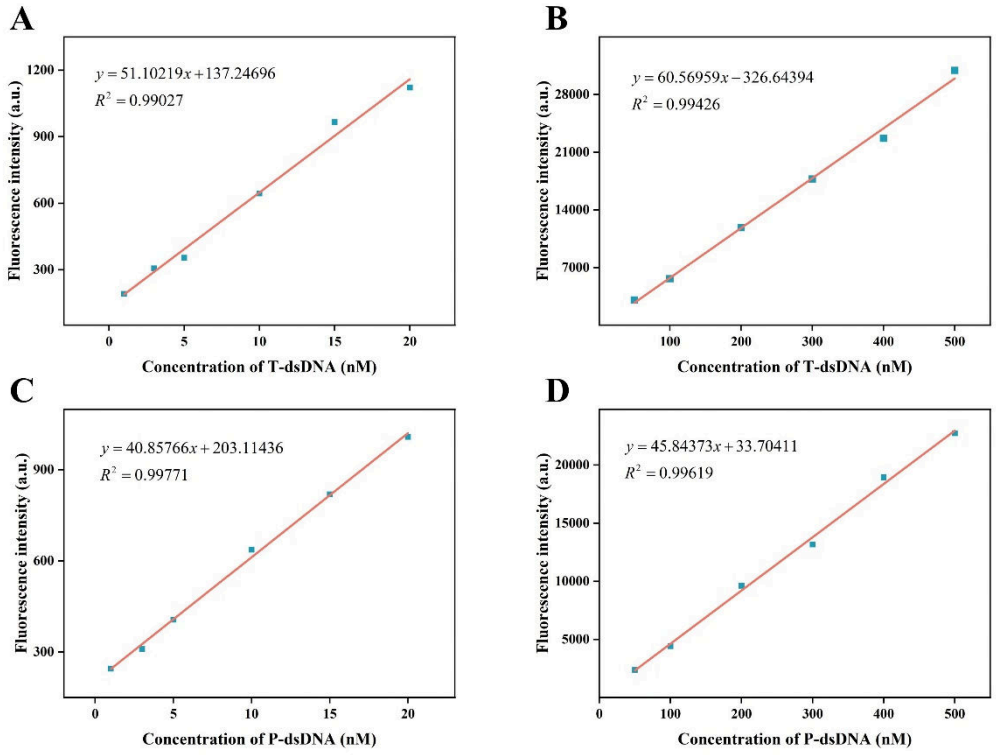


Figure S2. The linear plot of fluorescence intensity versus the concentration of T-

dsDNA or PAM-richer.

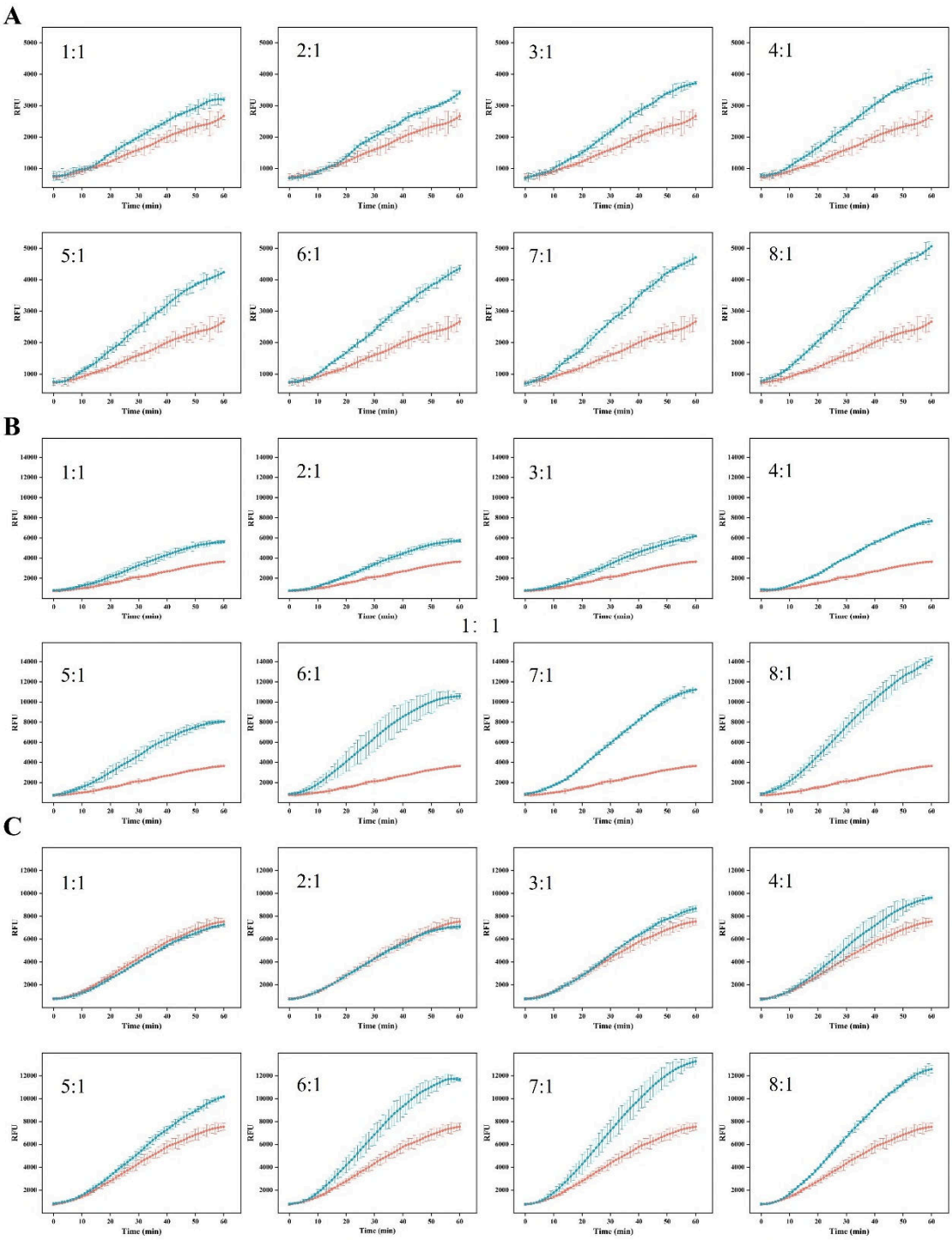


Figure S3. Real-time fluorescence curves of the reaction in the presence and absence of sPAM-antenna with different densities and proportions (ratio of PAM-richer to activator dsDNA). (A) Low density, (B) middle density, and (C) high density.

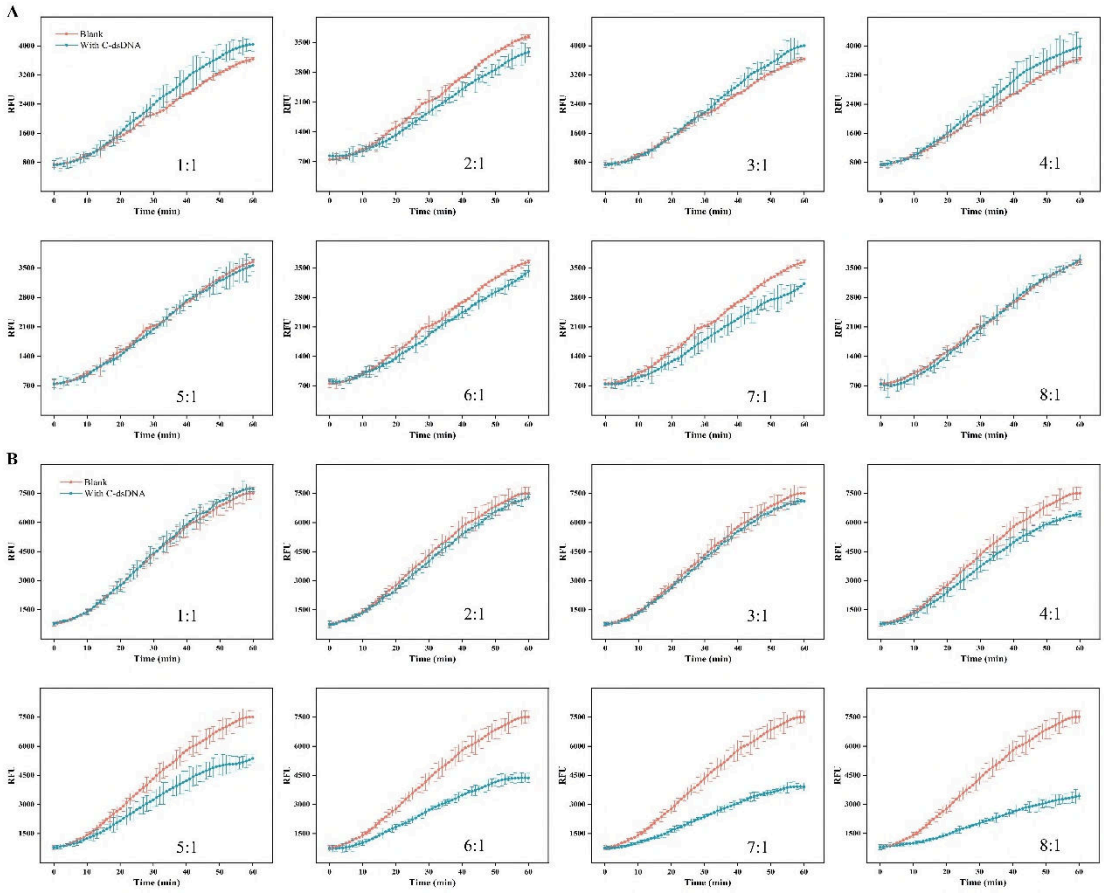


Figure S4. Real-time fluorescence curves of the reaction in the presence and absence of C-dsDNA with different densities and proportions (ratio of C-dsDNA to activator dsDNA). (A) Middle density and (B) High density.

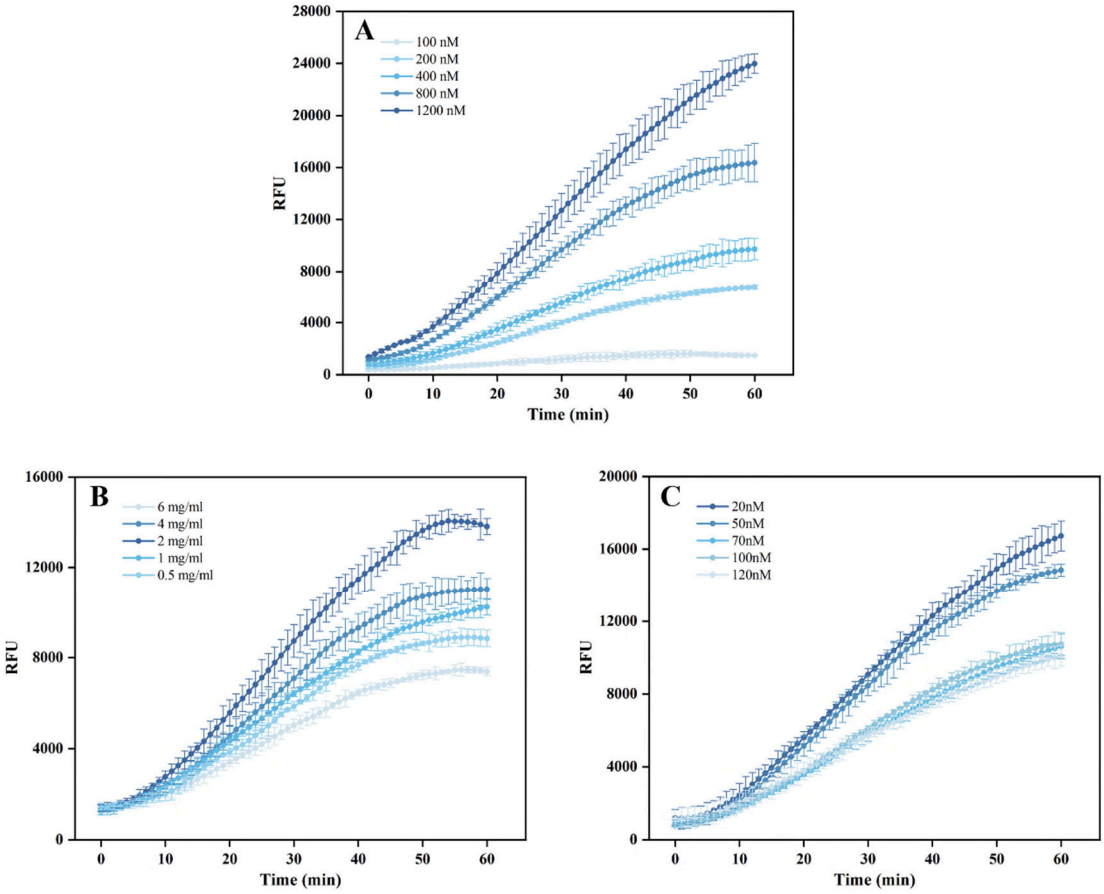


Figure S5. Optimization of the experimental conditions: the concentration of (A) FQ-reporter (B) Cas12a protein and (C) MBs.

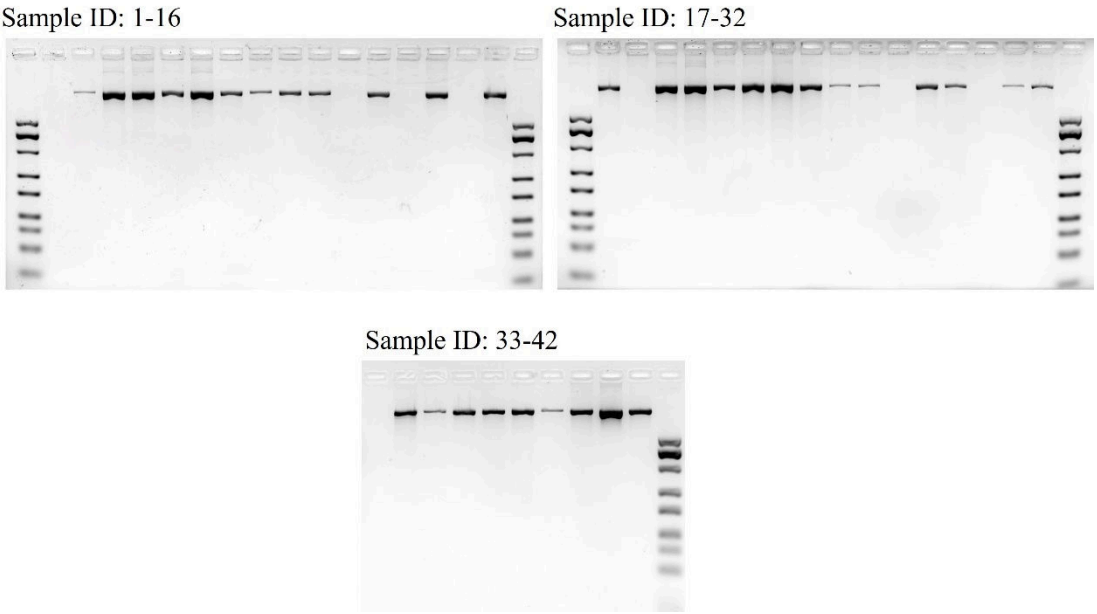


Figure S6. PCR results of 42 clinical samples.

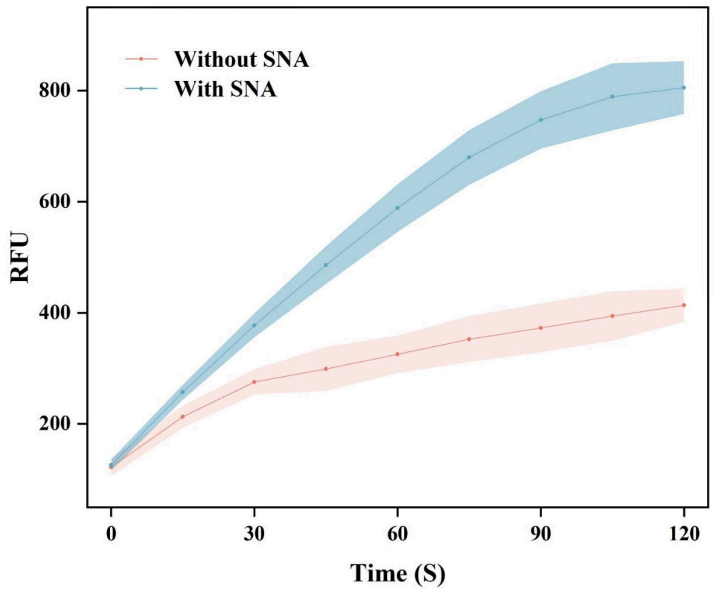


Figure S7. The influence of SNA on the hybridization rate between hairpin and target sequence.

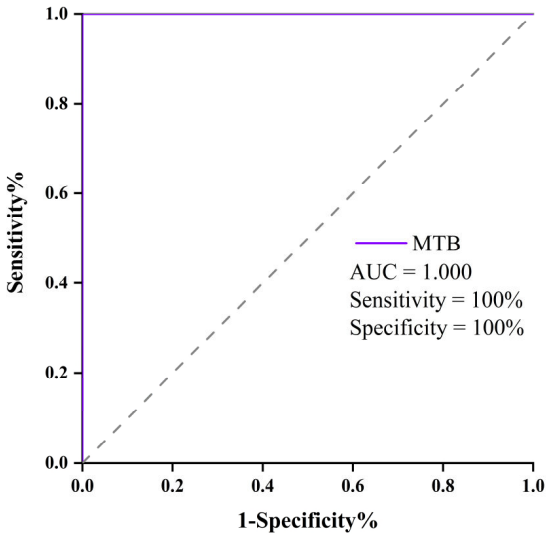


Figure S8. ROC curve analysis of spherical PAM-antenna enhanced CRISPR-Cas12a system detection accuracy in clinical applications

References

(1) Fu, X.; Shi, Y.; Peng, F.; Zhou, M.; Yin, Y.; Tan, Y.; Chen, M.; Yin, X.; Ke, G.; Zhang, X. B. Exploring the Trans-Cleavage Activity of CRISPR/Cas12a on Gold Nanoparticles for Stable and Sensitive Biosensing. *Anal. Chem.* **2021**, *93* (11), 4967-4974.

(2) Zeng, M.; Ke, Y.; Zhuang, Z.; Qin, C.; Li, L. Y.; Sheng, G.; Li, Z.; Meng, H.; Ding, X. Harnessing Multiplex crRNA in the CRISPR/Cas12a System Enables an Amplification-Free DNA Diagnostic Platform for ASFV Detection. *Anal. Chem.* **2022**, *94* (30), 10805-10812.

(3) Zhang, T.; Li, H. T.; Xia, X.; Liu, J.; Lu, Y.; Khan, M. R.; Deng, S.; Busquets, R.; He, G.; He, Q.; et al. Direct Detection of Foodborne Pathogens via a Proximal DNA Probe-Based CRISPR-Cas12 Assay. *J. Agric. Food. Chem.* **2021**, *69* (43), 12828-12836.

(4) Yu, T.; Zhang, S.; Matei, R.; Marx, W.; Beisel, C. L.; Wei, Q. Coupling smartphone and CRISPR–Cas12a for digital and multiplexed nucleic acid detection. *AlChE J.* **2021**, *67* (12).

(5) Yue, H.; Shu, B.; Tian, T.; Xiong, E.; Huang, M.; Zhu, D.; Sun, J.; Liu, Q.; Wang, S.; Li, Y.; et al. Droplet Cas12a Assay Enables DNA Quantification from Unamplified Samples at the Single-Molecule Level. *Nano Lett.* **2021**, *21* (11), 4643-4653.

(6) Lee, Y.; Choi, J.; Han, H.-K.; Park, S.; Park, S. Y.; Park, C.; Baek, C.; Lee, T.; Min, J. Fabrication of ultrasensitive electrochemical biosensor for dengue fever viral RNA Based on CRISPR/Cpf1 reaction. *Sens. Actuators, B* **2021**, *326*.

(7) Zhao, K.-R.; Wang, L.; Liu, P.-F.; Hang, X.-M.; Wang, H.-Y.; Ye, S.-Y.; Liu, Z.-J.; Liang, G.-X. A signal-switchable electrochemiluminescence biosensor based on the integration of spherical nucleic acid and CRISPR/Cas12a for multiplex detection of HIV/HPV DNAs. *Sens. Actuators, B* **2021**, *346*.

(8) Dai, Y.; Somoza, R. A.; Wang, L.; Welter, J. F.; Li, Y.; Caplan, A. I.; Liu, C. C.

Exploring the Trans-Cleavage Activity of CRISPR-Cas12a (cpf1) for the Development of a Universal Electrochemical Biosensor. *Angew Chem Int Ed Engl* **2019**, *58* (48), 17399-17405.
(9) Suea-Ngam, A.; Howes, P. D.; deMello, A. J. An amplification-free ultra-sensitive electrochemical CRISPR/Cas biosensor for drug-resistant bacteria detection. *Chem. Sci.* **2021**, *12* (38), 12733-12743.
(10) Zhang, D.; Yan, Y.; Que, H.; Yang, T.; Cheng, X.; Ding, S.; Zhang, X.; Cheng, W. CRISPR/Cas12a-Mediated Interfacial Cleaving of Hairpin DNA Reporter for Electrochemical Nucleic Acid Sensing. *ACS Sens.* **2020**, *5* (2), 557-562.



https://dspace.org/

Exploiting the potential of spherical PAM antenna for enhanced CRISPR-Cas12a: a paradigm shift toward a universal amplification-free nucleic acid test platform

Dai, Jiahui; Wu, Beibei; Ai, Fengxiang; Yang, Zhugen; Lu, Yanyan ...

2025-01-21
American Chemical Society
https://doi.org/10.1021/acs.analchem.4c04871
Dai J, Wu B, Ai F, et al., (2025) Exploiting the potential of spherical PAM antenna for enhanced CRISPR-Cas12a: a paradigm shift toward a universal amplification-free nucleic acid test platform. Analytical Chemistry, Volume 97, Issue 2, January 2025, pp. 1236-1245

Downloaded from a DSpace repository. https://dspace.org/